The Journal of Chemical Physics

RESEARCH ARTICLE | SEPTEMBER 21 2022

Derivable genetic programming for two-dimensional colloidal materials

Nathan A. Mahynski ; Bliss Han ; Daniel Markiewitz ; Vincent K. Shen

J. Chem. Phys. 157, 114112 (2022)
https://doi.org/10.1063/5.0106131
CHORUS

AIP Publishing

The Journal of Chemical Physics ARTICLE scitation.org/journal/jcp

Derivable genetic programming for two-dimensional colloidal materials

Cite as: J. Chem. Phys. 157, 114112 (2022); doi: 10.1063/5.0106131
Submitted: 27 June 2022 • Accepted: 21 August 2022 •
Published Online: 21 September 2022

Nathan A. Mahynski,[a] Bliss Han, Daniel Markiewitz, and Vincent K. Shen

AFFILIATIONS

Chemical Sciences Division, National Institute of Standards and Technology, Gaithersburg, Maryland 20899, USA

[a]Author to whom correspondence should be addressed: nathan.mahynski@nist.gov

ABSTRACT

We describe a method for deriving surface functionalization patterns for colloidal systems that can induce self-assembly into any chosen periodic symmetry at a planar interface. The result is a sequence of letters, $s \in \{A, T, C, G\}$, or a gene, that describes the perimeter of the colloidal object and programs its self-assembly. This represents a genome that is finite and can be exhaustively enumerated. These genes derive from symmetry, which may be topologically represented by two-dimensional parabolic orbifolds; since these orbifolds are surfaces that may be derived from first principles, this represents an *ab initio* route to colloid functionality. The genes are human readable and can be employed to easily design colloidal units. We employ a biological (genetic) analogy to demonstrate this and illustrate their connection to the designs of Maurits Cornelis (M. C.) Escher.

Published by AIP Publishing. https://doi.org/10.1063/5.0106131

I. INTRODUCTION

Self-assembled colloidal systems contribute to numerous modern technologies including photonic devices and sensors,[1] pharmaceutical delivery methods,[2–5] and designer framework materials for chemical separations or material organization.[6–10] Many applications rely on the assembly of a periodic two-dimensional (2D) film, e.g., to act as a reactive surface or size- or shape-selective barrier. Colloidal systems are chemically malleable enough that the constituent particles can be designed to self-assemble into a desired pattern; however, these designs are usually either bespoke, or they are sought after computationally, often via inverse design methods.[11–13] The former tends to require expert knowledge of individual systems, while the latter can yield interactions that are difficult to achieve in practice.[14] Regardless, all complex designs come with their own set of practical challenges. The connection between a particle's features and the structure or symmetry of the resulting self-assembled crystal remain poorly understood; thus, a direct mathematical derivation or *a priori* design of such features is typically out of reach, though recent work has sought to apply *ab initio* methods to hard particle systems that self-assemble based purely on entropy.[15] Here, we illustrate a derivable path from first principles to enthalpic colloid functionality composed of only short-ranged interactions, overtly encoded as a "genetic" sequence.

To achieve this, we use isohedral (IH) tilings of the 2D plane as templates to describe the perimeter of the colloid. Isohedral tilings are uniquely linked to crystallographic symmetry and have the remarkable property that their perimeters may be described as a set of matching segments, typically in pairs.[16] Different patterns of segments are uniquely associated with different wallpaper groups. Importantly, there are a finite number of IH tiles in two Euclidean dimensions.[16,17] A subset of these tiles describe fundamental domains (FDs), or asymmetric units, of crystals; these units contain the nonredundant portion of the pattern, and the crystal is formed by repeatedly duplicating the FD in a specific fashion for each wallpaper group.[16,18]

Here, we consider the problem of how to functionalize the surface of colloidal particles in a one-component system such that it will self-assemble into a periodic 2D film with specified symmetry. By considering asymmetric colloids to be the FD of a crystal, we demonstrated that these tiles can be used to define a circumscribing "ring" around the colloid that rationally programs their self-assembly.[19] Here, we provide an alternative route to guiding self-assembly by showing how symmetry can be used to derive surface functionalization patterns for these colloids resulting in "patchy" particles instead (cf. Fig. 1). In principle, this may be any colloidal object, such as a nanoparticle or protein, and this rational programming induces assembly into a functional interface, such as a structured monolayer

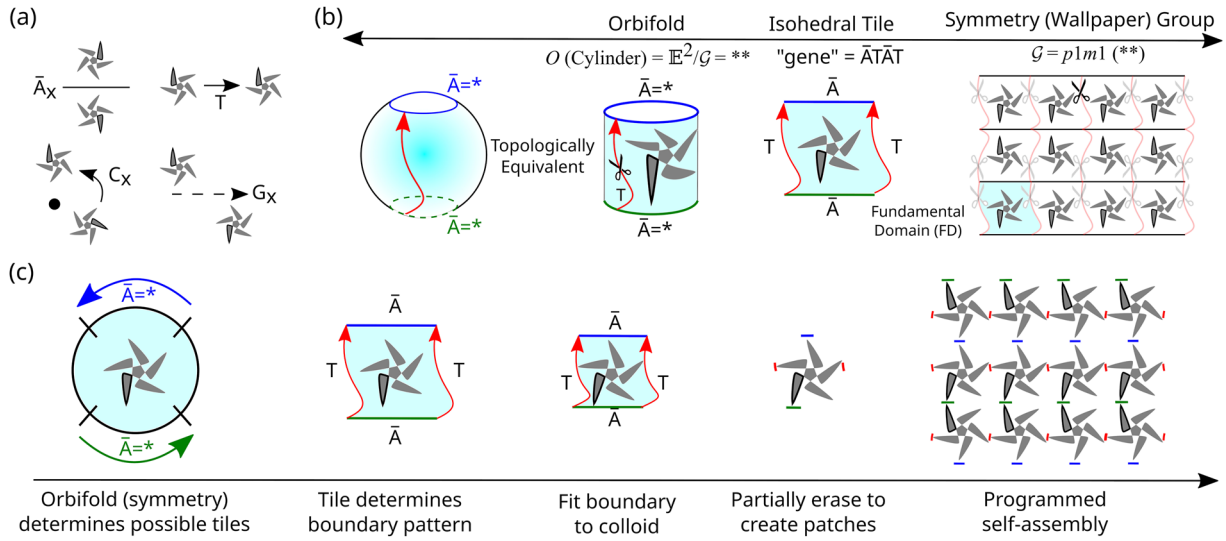

FIG. 1. Symmetry-based design concept. (a) The four isometries of the Euclidean plane ($\mathbb{E}^2$): reflection ($\bar{A}_x$), translation (T), rotation (C_x), and glide reflection (G_x), which is a combination of reflection and translation. (b) The connection between a surgically manipulated sphere, topologically equivalent to the orbifold, and how it may be "cut" open to produce an isohedral tile (IH) that is the FD of a crystal. (c) Summary of the colloidal functionalization scheme proposed in this work.

or porous membrane, with a chosen wallpaper group. In practice, we anticipate this approach may enable novel, intuitive design schemes for various technologies; for example, to create self-assembling films or membranes with easily programmable porosity for size-selective separations. Although high fidelity, large-scale manufacturing of patchy particles is an outstanding practical challenge, numerous technologies including peptidic,[20–22] DNA-based,[6,9,23–28] and small-molecule-based methodologies[29] offer promising pathways to these ends. As in previous work, we restrict ourselves to the assembly of asymmetric objects, while extensions to colloids with symmetry (such as a mirror plane) will be addressed in future work, as this framework is extensible to those cases.

This article is organized as follows. First, we review relevant background concepts for the derivation in Sec. II. In Sec. III, we demonstrate how boundary shapes and patterns follow directly from a given wallpaper group in an *ad hoc* fashion and their genetic labeling scheme. Section IV illustrates how to subsequently imprint this information on the surface of the colloidal unit and other features. We conclude this article in Sec. V.

II. BACKGROUND

Orbit manifolds, or orbifolds, play a central role in our approach. Orbifolds are surfaces that may be derived from the surface of a sphere and can be used to describe 2D symmetry groups.[30–32] Importantly, they connect concepts from symmetry, crystallography, and tiling in an intuitive way by a process of "cutting" and "glueing," making the results easily interpretable and practical to use.[33,34] In our view, this result is not very well known and is an underutilized tool in the rational design of soft matter systems. Section III presents a shortcut that enables practitioners to apply this method without a specialized background in these subjects.

A. Orbifolds and symmetry

Two-dimensional symmetry groups, or wallpaper groups, describe unique combinations of operations, known as isometries, which duplicate the FD of the pattern to tessellate the plane. There are four isometries of the Euclidean plane, $\mathbb{E}^2$: translation, rotation, reflection, and glide reflection—which are shown in Fig. 1(a) and denoted by letters that will be explained later. A topological approach to describing the combinations of these isometries that form valid crystallographic groups is due to the work by Thurston and Conway,[30,31] which involves performing "surgery" to encode these operations on a sphere. Each surgery removes some curvature from the sphere and, by virtue of the Gauss–Bonnet theorem, reduces the Euler characteristic, χ, as well.[35] Conway's "magic theorem"[34] states that those surfaces that have $\chi = 0$ correspond to valid groups acting in the Euclidean plane, which are known as parabolic orbifolds.[30] Thus, orbifolds may be derived directly from the surface of a sphere. This is topologically equivalent to folding up a FD for a crystal[36] to match symmetrically equivalent positions, and the orbifold is unique for each group.[31]

Figure 1(b) shows a sphere with one hole punched at each of its poles to encode two mirror planes, corresponding to the $p1m1$ wallpaper group. The supplementary material, Sec. S1, contains a brief summary of Conway's orbifold naming scheme, which represents these features with a ring (o), numbers before an asterisk, asterisk(s) followed by numbers, and × symbols to denote translations, rotations, reflections, and glide reflections, respectively. More details are available elsewhere.[31,32,34] Thus, the orbifold designation for $p1m1$ is ** and is topologically a cylinder.

These orbifolds, O, may be viewed as topological quotients of the space they model by its wallpaper group.[30,32] Here, we focus on $\mathbb{E}^2$, whose symmetries are described by 1 of the 17 wallpaper groups, $\mathcal{G}$,

$$\frac{\mathbb{E}^2}{\mathcal{G}} \overset{\text{Disassemble}}{=} O. \tag{1}$$

We may imagine the manifestation of this mathematical division as the physical division of the plane (cutting) with a pair of scissors such that its symmetric copies collectively cut in a way that results in pieces [a FD, cf. Fig. 1(b) shown in cyan] such that they are all equivalent and any pair may be mapped to each other by actions of the group. Enumerating all possible ways to reverse this tile-folding process by cutting open an orbifold yields all topologically distinct IH tiles that are fundamental domains of a given group.[33,34] Figure 1(b) shows the orbifold for $p1m1$ (**) is a cylinder that may be cut from one end to the other to be unfolded into a FD, which is an IH tile, for this group. Note how the scissor's path (red arrow) is essentially arbitrary as long as it does not intersect itself, which would lead to multiple pieces. Another example is provided in the supplementary material, Sec. S2.

These IH tiles are the philosophical basis of our design procedure because Eq. (1) suggests we may view the programming necessary to induce self-assembly as the product of the orbifold and the group; if the latter is specified by the designer, the properties to achieve it are encoded in the former,

$$O \times \mathcal{G} \overset{\text{Assemble}}{=} \mathbb{E}^2. \tag{2}$$

In previous work, we examined the features of these tiles that give rise to different self-assembly characteristics and categorized them on this basis.[19] In that case, the tiles are considered structure directing rings, whose perimeter curvature is critical to unambiguously encode the pattern's correct self-assembly.

Here, we consider the case where this information becomes only partially imprinted around the colloid, as surface functionalization, resulting in a "patchy particle" [cf. Fig. 1(c)]. This may be easier to achieve in practice and is more compatible with current design and synthesis practices; however, this effectively deletes a significant amount of programming information relative to the complete ring. To compensate for this, we must expand our "genetic" design, described next, to include the concept of "stop codons," which is the main consequence of this design change.

B. A genetic encoding

Orbifolds enable material genomes[37] to be derived for hypothetical three-dimensional crystalline materials such as zeolites and metal–organic frameworks.[38–41] This entails systematically subdividing and recombining a crystal's FD to produce different detailed tilings; however, in this work, we assume the predefined colloidal unit will occupy interior of the FD (isohedral tile), precluding any division, which greatly simplifies the resulting "genome."

Other mathematical tools, besides orbifolds, were first used to exhaustively enumerate topologically distinct isohedral tiles that are crystalline FDs; there are 46 in total.[16] However, in our view, the explanation[33] that these 46 tiles result from cutting open the 17 parabolic orbifolds describing wallpaper groups is the most intuitive, and it visually reveals how to "extract" the self-assembly information we are seeking. The IH tiles are formed by the cutting process exemplified in Fig. 1(b), which must cut the orbifold into a single, flat piece with no internal rotation centers.[33,34] The tile's edge pairings result from being on either side of the scissors, and their shape is simply the path chosen. The cylinder in Fig. 1(b) can only be cut in the way shown to produce a valid FD, but most orbifolds can be cut in many different ways. Here, the cut results in a pair of edges that are translated (T) images of each other between the two mirror boundaries.

In general, edge pairs can be labeled using the same four isometries used to construct the wallpaper groups themselves. Historically, Heesch and Kienzle developed such a naming system for fully interlocking tiles before the development of modern orbifolds. This excludes groups with reflections, which create straight edges, and encompassed 28 out of the 46 tiles.[17] Their naming scheme labeled edges with a T, C_x, or G_x to denote translates, cycles (rotations), and glides, respectively. Paired edges are typically denoted by using the same letter; however, a subscript is added to glide pairs when multiple pairs occur to distinguish them from each other (e.g., $G_1G_2G_1G_2$). The subscript for cycles is different and, instead, denotes the order of rotation. By convention, an edge with a twofold rotation center (180°) has no subscript and pairs with itself about its midpoint; thus, it has no other paired letter in the sequence. Some examples and more details are provided in the supplementary material, Sec. S3.

Thus, a sequence of letters, $s \in \{\mathrm{T}, \mathrm{C}, \mathrm{G}\}$, results when the tile's perimeter is traversed in a fixed orientation (clockwise or counterclockwise) where matching letters imply symmetric equivalence (matching edges). Only seven wallpaper groups fall into this mirror-less category ($p2gg$, $p1g1$, $p1$, $p2$, $p3$, $p4$, $p5$, $p6$), which can easily be identified as all groups whose orbifold symbol contains no asterisk. Reference 42 has expanded the naming scheme to include reflections, or axis mirroring ("Achsenspiegelung" in German), represented by an "S" ("Spiegel" is the German word for mirror); however, this system does not cover all 46 tiles distinctly. Moreover, the naming scheme is more descriptive than prescriptive, that is, the shape of the tile cannot be entirely inferred from the name alone—for example, to describe how mirrors shoul intersect. Here, we expand Heesch and Kienzle's original notation with an "$\overline{\mathrm{A}}_x$" instead. The overbar emphasizes the edge must be straight [cf. Fig. 1(a)], unlike others. If mirrors meet at an angle of π/x, a subscript of x is added; otherwise, there is no constraint on the angle at which a mirror meets a neighboring edge in our system. Thus, the perimeter of a tile can be represented by a sequence of letters, $s \in \{\mathrm{A}, \mathrm{T}, \mathrm{C}, \mathrm{G}\}$. As we will show, however, the genetic analogy goes beyond this superficial lettering.

Independently, the Dutch artist Maurits Cornelis (M. C.) Escher discovered 27 out of the 28 original Heesch types.[43] He also explored other symmetries, but he primarily focused on these since mirror planes were considered less interesting and less common in the natural motifs he focused on.[43,44] He developed a theory for the "regular division of the plane" ("regelmatige vlakverdeling") inspired by crystallography[43] that is precisely analogous to the division in Eq. (1); while his final works typically contained many design elements, his motifs were often based on isohedral tilings, which can be labeled according to this genetic scheme.[43] The diversity and complexity that Escher's artwork illustrates are precisely inherited by our design approach as a superset of Heesch's system.

III. METHODS

Next, we describe a simple shortcut to obtain permissible shapes for the FD (different IH tiles) of each wallpaper group using only its orbifold signature, which is the first step in obtaining the surface functionalization pattern. Importantly, there is not just one single shape for a given wallpaper group but families of them; all members of the same family have the same number of edges and pattern of pairwise edge relationships, but they may have very different edge lengths, curvatures, and certain angles. Variations within a family essentially represent different valid paths the scissors may follow along a cut [cf. red path in Fig. 1(b)], whereas variations between different families represent different choices of cuts that can be made on the orbifold;[33,34] our shortcut is essentially an incomplete approximation of an exhaustive enumeration of these processes. This shortcut's utility derives from its simplicity, which streamlines our design approach for the practitioner.

A. A shortcut

First, draw a circle to topologically represent the boundary of the crystal's FD (equivalent to an unfolded orbifold), as in Fig. 1(c); next, decorate it with Conway's orbifold symbols representing the group's isometries (cf. supplementary material, Sec. S1). If we envision the ring as being discretized into points, we can then assign each point to one, and only one, of the elements. Once the ring is decorated, we divide the space between the elements leaving no gaps so that all points are assigned to a symmetry element. Symmetry operations act about these elements to map points to their symmetrically equivalent ones as follows:

1. Rotations (numbers preceding an asterisk) must own equal distances on either side of the center, since they map one side onto the other, creating a palindromic copy about the center. They also require that its two sides meet at an angle of $2\pi/N$ for an Nth-order rotation. The area between the two sides corresponds to the "inside" of the tile and the must be oriented accordingly.
2. Mirrors (asterisks) create straight lines, and corner points (denoted by numbers following an asterisk, $^{*}n$) are formed by mirrors that intersect at an angle of π/n. If multiple mirrors are present that do not form a corner point (**), they are parallel (nonintersecting) as shown in Fig. 1(b).
3. Glides (denoted by ×) form "V" shapes where each side is an edge, and they are connected without any gap between them. Naturally, this implies the edges have equal length and create a sequence that repeats itself after the vertex.

Any variable that is not defined by these elements may be arbitrary. The only constraints are that the ring (1) must close, (2) have finite area, and (3) possess no overlapping edges, so that it forms a so-called "normal" tiling.[16,45] We are free to adjust any angle, edge curvature, or length so long as the ring satisfies these requirements, and its shape will be a valid FD for the wallpaper group in question. Note that the distance along the ring assigned to an element may be any non-negative value, including zero. Additional details can be found in the supplementary material, Sec. S4.

An example for the *p2gg* (22x) group is shown in Fig. 2. L_A (blue) is some distance to one side of a twofold rotation center, as is L_B (green). L_C (magenta) refers to the length of an edge that is mapped by a glide operation to a connected copy. All edges are given arrows to denote direction. While construction may start from any point, Fig. 2(b) begins with a twofold rotation center by drawing an arbitrary nonintersecting curve and rotating it 180° (Step 1); this is repeated for the second twofold rotation center (Step 2). These segments can be then connected at any angle, but they must form a closed ring when combined with the glide pair (Step 3). Applying these operations to match edges on duplicates of the tile creates a tessellation belonging to the *p2gg* wallpaper group.

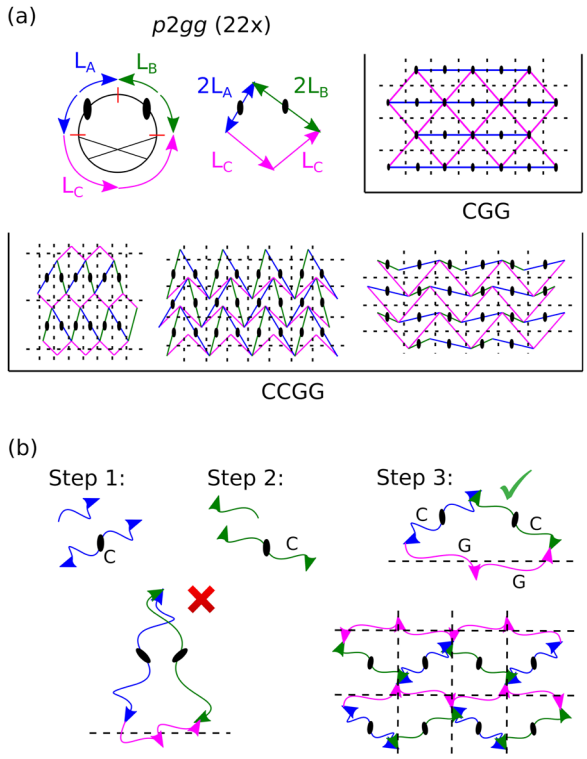

FIG. 2. Deriving the shape of a FD for a wallpaper group. (a) Example placement of the *p2gg* (22x) group's symmetry elements on a ring (two 2-fold rotations and a glide reflection); the elements are divided by red bars. There are two topologically distinct FDs that can be found. Several examples for the first topological type (CCGG) are shown and one for the second (CGG). (b) Steps are explicitly shown to construct an example CCGG tile. A correct and incorrect result from Step 3 are shown.

Note that it is possible to have any angle between any of the differently colored segments because no symmetry element determines them. The only angle that is fixed is directly on the rotation centers (180°). Three different CCGG examples are shown in Fig. 2(a). Moreover, it is possible to set either L_A or L_B to zero since it is possible to make a ring with the magenta (glide) portion and the nonzero one (CGG tile). Conversely, it is not possible to set $L_C = 0$ because a closed, nonoverlapping ring encircling a finite area cannot be constructed out of the two segments corresponding to the rotation centers. More details are available in the supplementary material, Sec. S4.

Figure 3 illustrates an example of a decorated ring for each wallpaper group. The supplementary material, Sec. S5, contains a

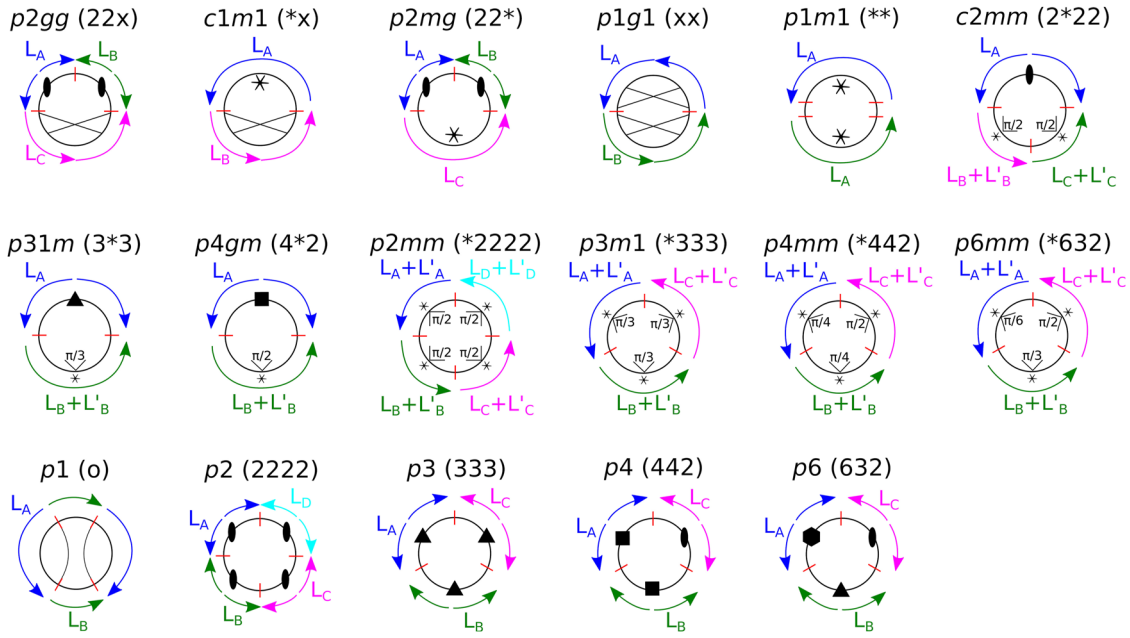

FIG. 3. A complete list of fundamental domains of two dimensional crystals that can be derived via the shortcut method described in the text. This is a brief summary of the start of the derivation for all possible tiles for each group. *N*-fold rotation centers are denoted by regular *n*-gons (2-fold centers are ellipses), a glide by an "X" (crossed lines), and a mirror by an asterisk. Corner points are further decorated with a wedge and the angle that occurs there. In those cases, there is some length allowable before (e.g., L_A) or after (e.g., L'_A) the corner, which are independent of each other.

complete list of examples and the different tiles that result from this shortcut procedure by varying lengths of different edges. Overall, this generates 28 out of the 46 possibilities; 11 of the 17 groups are exhaustively enumerated this way, while the remaining 6 have at least one instance but not all possibilities. This is essentially a consequence of the fact that (1) it is not necessary to assign each point on the ring to one of these elements and (2) glides do not necessarily need to operate about a gap-less vertex as we have specified. Relaxing these restrictions enables one to generate the remaining domains; however, it requires additional considerations to determine what the nature of these "gaps" should be and where they are allowed. In general, these gaps are almost always translation pairs, though for groups with (glide) reflections, it is possible for additional (glide) reflections to manifest.

This emphasizes the direct connection between boundary condition and symmetry. In molecular simulations, "standard periodic boundary conditions"[46] used to simulate systems with as little imposed symmetry as possible belong to the *p*1 group, and they are considered "toroidal" because of the shape of the orbifold.

B. A complete genome

We may regard topologically distinct FDs that belong to the same wallpaper group, e.g., CCGG vs CGG, as "isotopes" of each other since they derive from the same topological object (orbifold). While these are not related by a formal topological isotopy,[16,34] these tiles can be continuously transformed into each other by adding or removing edges. These appear closely related to Escher's "transitional" systems—he used to derive new tile types by pivoting parts of another tile's boundaries.[43,47] Similarly, Heesch and Kienzle described nine "core types" (Haupttypen) for groups without reflections that represent primary tiles from which the others are derived by removing edges, e.g., $L_B \to 0$ changes CCGG to CGG in Fig. 2(a).[17,48]

We have constructed networks to illustrate transitions between all fundamental domains for all wallpaper groups. Figure 4 illustrates this network for the group with the most topologically distinct tiles, *p2gg* (22x). The two possible tiles, both derived in Fig. 2, are shown in black boxes. Qualitative instructions are provided along with arrows to indicate the direction of incremental transitions. A network for each group is available in the supplementary material, Sec. S6. This graphically demonstrates how tiles (genes) derived from our shortcut method can be continuously transformed to yield all possible tiles (genes) for a given group. Note that these isotopes may exhibit differences in self-assembly behavior (pathways), even if the group is the same as explored in Ref. 19.

Table I lists all tiles and associated genes that form fundamental domains of crystals. Blue entries denote those that are derived from our shortcut method. Observe that all other genes for a given group are created by a combination of deleting some pairs of matching letters and by possibly adding some translate pairs (T) or edges involving reflection ($\bar{A}$ or G), as noted in Sec. III A. We emphasize that while this naming scheme uses similar characters as in DNA code, here we do not have an analogous base-pairing (e.g., A with T); instead, all edges pair with copies of themselves, e.g., G with another G.

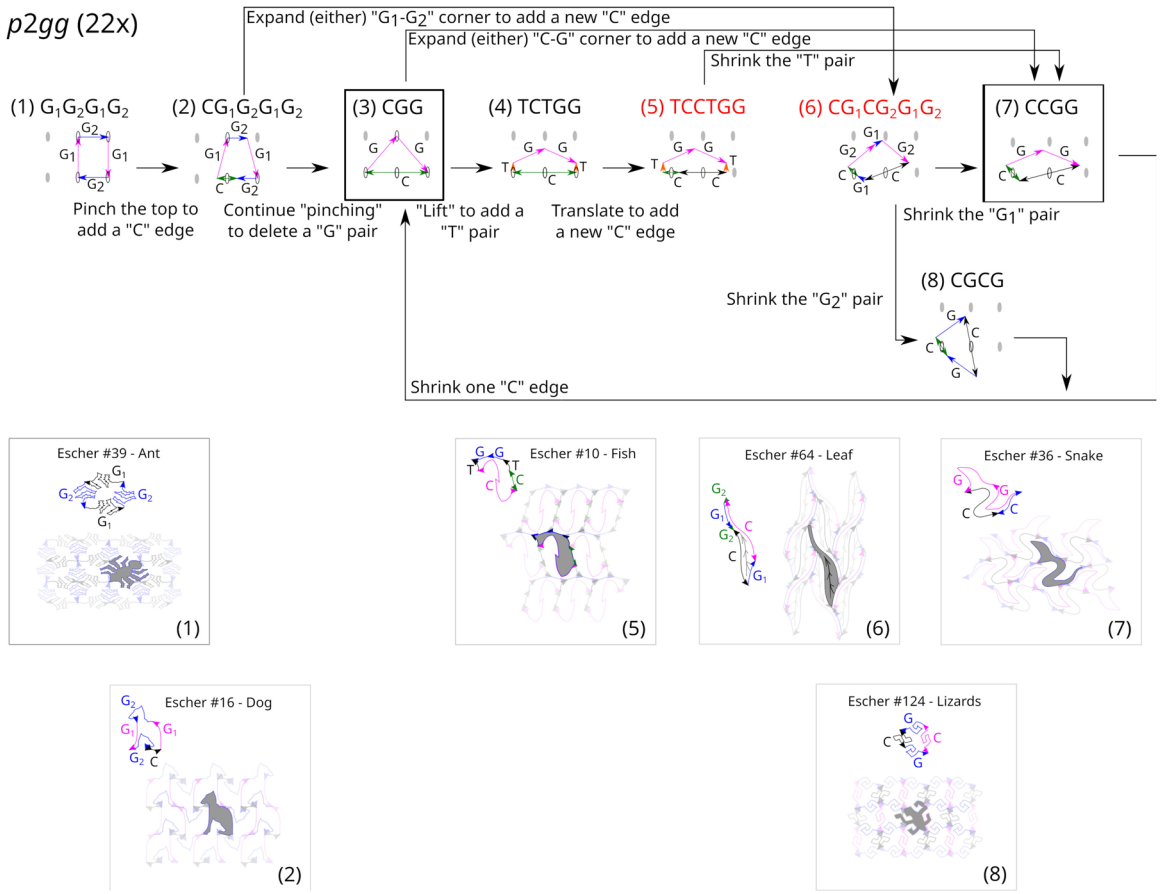

FIG. 4. The *p2gg* (22x) group is defined by perpendicular glide lines (not depicted) with twofold rotations centered in the rectangles these lines trace out. Heesch and Kienzle's "core types" are listed in red, for reference. Numbers in parentheses are specific to this work and are used to number the FDs from 1 to 46. Numbers 3 and 7 are boxed to indicate that they can be derived from the shortcut method presented in Fig. 2. Transformations are described qualitatively in the direction of the black arrows, which may simply be reversed to go in the opposite direction. Gray boxes below contain examples of these tiles reproduced from Escher's folios.[43]

C. Simulations

Two-dimensional canonical molecular dynamics (MD) simulations were performed using the LAMMPS package.[49] Functionalized colloids were created as rigid bodies by decorating a central sphere with smaller spheres of diameter, $\sigma = 1$. These decoration spheres were assigned an identity based on symmetry. Symmetrically equivalent sites received the same identity and interacted favorably via a cut-and-shifted Lennard-Jones-like potential: $U = U_{\mathrm{LJ}}(r) - U_{\mathrm{LJ}}(r_c) - (r - r_c)\frac{\partial U}{\partial r}|_{r_c}$,[50] with

$$U_{\mathrm{LJ}}(r) = \begin{cases} 4\varepsilon\left(\left(\frac{\sigma}{r}\right)^{2n} - \left(\frac{\sigma}{r}\right)^{n}\right), & r \le r_c, \\ 0, & r > r_c, \end{cases} \tag{3}$$

where $\varepsilon = 1$ and $n = 9$. All quantities were non-dimensionalized in terms of the σ and ε. Interactions between unlike points and with "stop codons" (a decoration explained in Sec. IV A) were truncated at $r_c = 2^{1/n}\sigma$ so that they were purely repulsive; attractive interactions were truncated at $r_c = 3.0\sigma$. Central cores similarly interacted in a purely repulsive manner. Once decorations were placed, they were scaled to contact and the core's diameter, σ_c, was set to nest inside of these points. Typically, $\sigma_c \approx 7\sigma$. A Langevin thermostat was used with a damping constant of $d = 10$; the mass of each particle was set to $m = 1$ and the time step was set to $\delta t = 0.005$.

We defined an approximate surface coverage, $\rho = \sqrt{\frac{\pi\sigma_c^2 N_{\mathrm{tot}}}{L^2}}$, where L is the edge length of the square simulation cell. We typically chose $\rho = 0.66$ and computed L from this. We usually set the simulation temperature to $T^* = k_{\mathrm{B}}T/\varepsilon = 0.25$, where k_{B} is the Boltzmann constant. A racemic system of $N_{\mathrm{L}} = N_{\mathrm{D}} = 50$ ($N_{\mathrm{tot}} = 100$) was initialized on a lattice, then randomized using only repulsive interactions for all points for 1×10^6 steps; the attractive interactions were enabled and the system was evolved for up to 5×10^8 more steps until the system's total pairwise potential energy reached a constant value. For the *p6* example, which undergoes chiral phase separation, $N_{\mathrm{L}} = N_{\mathrm{D}} = 100$ ($N_{\mathrm{tot}} = 200$) was used instead.

TABLE I. A list of all genes for each wallpaper group. Groups bolded on the left correspond to those previously explored by Heesch and Kienzle and contain no reflections (mirrors).[17] Genes in blue derive directly from our shortcut method and are related to other black ones in the same group by a network akin to Fig. 4 (cf. supplementary material for a complete reference). The numbering scheme here is identical to that provided in Ref. 19, which translates them into the "IH" designation of Ref. 16.

Name	Orbifold description	Genetic sequence for all tiles
***p2gg* (22x)**	Non-orientable American Football	(1) $G_1G_2G_1G_2$, (2) $CG_1G_2G_1G_2$, (3) CGG, (4) TCTGG, (5) TCCTGG, (6) $CG_1CG_2G_1G_2$, (7) $CCGG$, (8) CGCG
*c*1*m*1 (*x)	Möbius band	(9) $\overline{A}G\overline{A}G$, (10) $\overline{A}GG$, (11) $\overline{A}TGGT$
*p*2*mg* (22*)	(Open) pillowcase, or Two-pointed hat	(12) $\overline{A}C\overline{A}C$, (13) $\overline{A}CC$, (14) $\overline{A}TCCT$, (15) $\overline{A}TCT$
***p1g1* (xx)**	Klein bottle	(16) $TG_1G_1TG_2G_2$, (17) $G_1G_1G_2G_2$, (18) $TG_1G_2TG_2G_1$, (19) TGTG
*p*1*m*1 (**)	Cylinder	(20) $\overline{A}T\overline{A}T$
*c*2 mm (2*22)	4,4,2 turnover with a slit along one edge (4,4)	(21) $\overline{A}_2\overline{A}_2\overline{A}C$, (22) $\overline{A}_2\overline{A}C$,
*p*31*m* (3*3)	6,3,2 turnover with a slit along one edge (6,2)	(23) $\overline{A}_3\overline{A}C_3C_3$, (24) $\overline{A}C_3C_3$
*p*4*gm* (4*2)	4,4,2 turnover with a slit along one edge (4,2)	(25) $\overline{A}_2\overline{A}C_4C_4$, (26) $\overline{A}C_4C_4$
*p*2*mm* (*2222)	Rectangle	(27) $\overline{A}_2\overline{A}_2\overline{A}_2\overline{A}_2$
*p*3*m*1 (*333)	Equilateral triangle	(28) $\overline{A}_3\overline{A}_3\overline{A}_3$
*p*4*mm* (*442)	Isosceles, right triangle	(29) $\overline{A}_4\overline{A}_4\overline{A}_2$
*p*6*mm* (*632)	Scalene, right triangle	(30) $\overline{A}_6\overline{A}_3\overline{A}_2$
***p1* (o)**	Torus	(31) TTTT, (32) TTTTTT
***p2* (2222)**	Closed, four-pointed pillowcase	(33) CCC, (34) CCCC, (35) TCCTCC, (36) TCTCC, (37) TCTC
***p3* (333)**	3,3,3 turnover (3-pointed pillowcase)	(38) $C_3C_3C_3C_3C_3C_3$, (39) $C_3C_3C_3C_3$
***p4* (442)**	4,4,2 turnover (3-pointed pillowcase)	(40) CC_4C_4, (41) $CC_4C_4C_4C_4$, (42) $C_4C_4C_4C_4$
***p6* (632)**	6,3,2 turnover (3-pointed pillowcase)	(43) CC_3C_3, (44) $CC_3C_3C_6C_6$, (45) CC_6C_6, (46) $C_3C_3C_6C_6$

IV. RESULTS AND DISCUSSION

A. Deriving surface functionality

We have now illustrated the path from orbifolds (symmetry) to families of FD shapes, and their genetic labels. Next, we will use these tiles to determine where and how to functionalize colloidal units. Each gene may be thought of as describing constraints on the shape of an elastic ring (cf. Fig. 3), which will be "shrinkwrapped" around the colloid, then partially erased. Depending on the shape of the colloid, one gene might be more natural to use than another. Escher exploited a related approach to create patterns of diverse motifs; some are illustrated in Fig. 4. While these may look very different, in fact, their tilings belong to the same wallpaper group. The diversity of his artwork illustrates the enormous range of particle shapes and sizes that can be accommodated by this approach.

In Ref. 19, we examined the assembly of complete tiles and characterized their self-assembly behavior based on what amounts to their gene sequence. In the case where symmetrically identical points attract each other, a nonzero curvature along a tile's edges is necessary to avoid defects arising from practical complications of planar assembly following deposition from a supernatant 3D environment. We would like to imprint a gene's information on the colloid's surface with as few points as possible for simplicity; however, this "maximum erasure principle" will eventually be limited by a lower bound (minimum amount of information) necessary to unambiguously encode self-assembly. Erasing nothing simply corresponds to the work in Ref. 19.

For illustration purposes, we adopt a simple anisotropically labeled circle in Fig. 5 as our colloidal unit and place it within a tile. The tile's perimeter may be divided into discrete points; while it is not necessary to erase the points on the tile far away from the colloid's surface (often, the tile's "corners" for convex colloids) and retain those that are closest, we expect this to be the most relevant for experimental realizations. Points tangent, or nearly so, to the colloid can then be chosen for functionalization, shown as differently colored spheres. This may require that some points project away from the surface to match an edge, which could be difficult to achieve in practice for some systems, though recently developed "stamping" methodologies may provide a pathway to this end.[27,28]

For colloidal units with soft coronas, such as polymer grafted nanoparticles and star polymers, we may envision a different interpretation of a "point." Figure 5(b) illustrates a representative "blob" model of such particles.[51,52] In this case, it is possible to make subsurface chemical modifications, i.e., to the inner green layer and not only the outer one. The tile may be viewed as transecting the corona, and the tile's points correspond to the blobs that intersect the perimeter. Regardless of the "hard" (a) or "soft" (b) interpretation, the tile itself determines where and how to decorate the colloid.

The interpretation of a "point" to functionalize will depend on the chemistry of the specific system, and we make no attempt to specialize to any particular system. Nevertheless, general guidelines for the minimum number of points needed may be obtained from simple arguments. First, observe that only two points are required to define a linear edge (needed for $\overline{A}_x$); however, as shown previously,[19] nonzero edge curvature is necessary to avoid defects from tiles that may rotate out of the assembly plane. Thus, for all non-mirrored edges (T, C_x, G_x), a third point is required that is not collinear with the other two. Second, while three points may suffice for a generic C_x edge, $C_2 = C$ is a special case. Here, a twofold rotation center exists in the middle of what might be considered a single edge, rather than a corner between a pair of them oriented at 180°. We may reduce the $3 \times 2 = 6$ total points to 4 by deleting the inner pair if we require

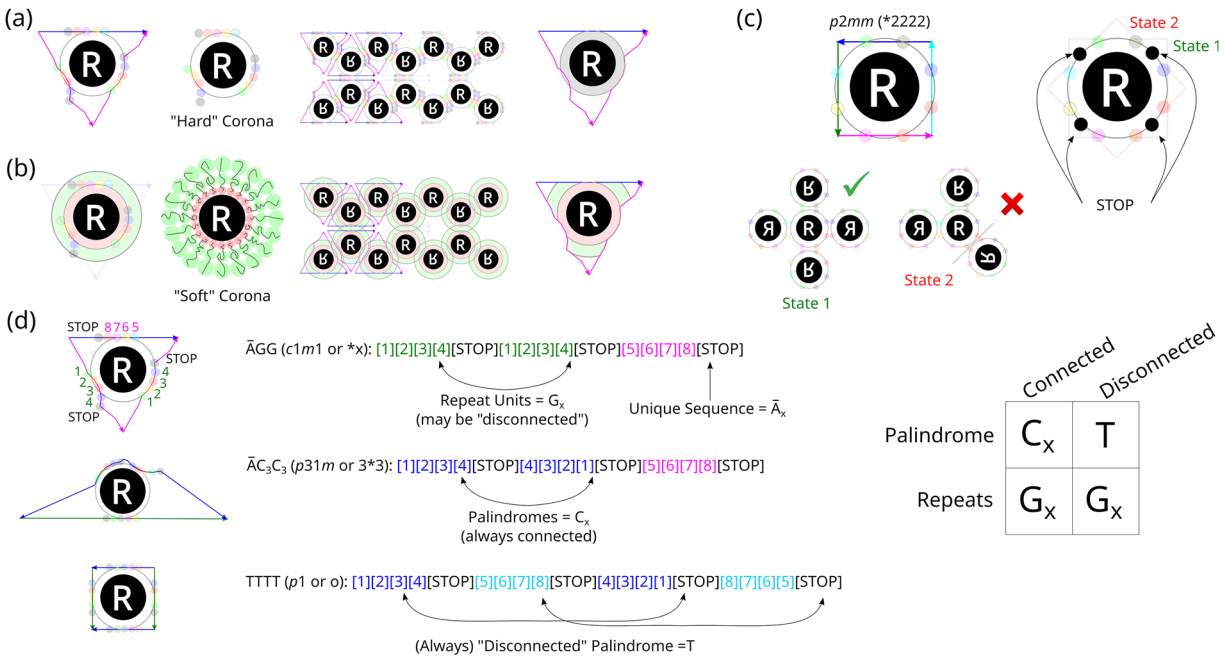

FIG. 5. Functionalizing a colloidal unit. Beads with the same color attract each other, while different colors do not. (a) The $\overline{A}GG$ ($c1m1$ group) tile is used to functionalize a hard surface (denoted with the letter "R" for illustration). (b) We could also view this as making subsurface modifications to the corona of a soft particle, such as a polymer-grafted nanoparticle. (c) "Stop codons" (black) can be used to prevent corner–corner interactions via steric hindrance. (d) Patterns of chemical identities on the colloid surface created by different tiles. The matrix at the right indicates the isometry that corresponds to a given pattern. Mirrors, $\overline{A}_x$, are a result of unique, non-repeated sequences.

the remaining 4 have nontrivial curvature symmetric about its midpoint. The supplementary material, Sec. S7, illustrates this argument explicitly.

Thus, the minimum number of sites to encode each edge is two, three, or four for mirrors ($\overline{A}_x$), non-mirrored edges that are not C, and C edges, respectively. After erasing points from the tile's corners inward to the colloid's surface, as in Fig. 5(a), consider that any two points at the ends of adjacent edges (e.g., green and black or cyan and black points) could pair with a tile of the opposite chirality. This would result if two colloids approached each other such that the corners of their inscribing tiles overlap, instead of making nonoverlapping edge–edge contact. As in previous work,[19] we assume that out-of-plane rotational diffusion of these systems will be inevitable in practice, creating a racemic mixture. Therefore, just as edge curvature becomes a practical requirement to avoid defective assembly from chiral mismatches, we must also make the system robust against these defects arising from "corner–corner" contact.

Figure 5(c) illustrates a pathological case when programming self-assembly with a square $p2$ mm tile ($\overline{A}_2\overline{A}_2\overline{A}_2\overline{A}_2$). It is possible for this system to assemble as intended (State 1), but it is also possible for a colloid to attach to the central one via a "corner" (State 2). In this particular case, if it happens at all four corners, the correct symmetry is actually obtained; this is equivalent to having programmed the system starting from a square rotated 45° relative to the one actually used. This creates two local configurational states that are energetically degenerate; thus, the system will generally exhibit both at random, inhibiting global order. This confusion is suppressed when the complete tile is used (no erasing) because the corners enforce the correct geometry sterically. This edge/corner confusion is the main penalty of erasing some of this edge information.

In our simulations, we found that using four points along all edges, regardless of type, provided enough of an energy gap between defects (2ε) and correct matches (4ε) to allow our systems to assemble well. This can be further improved by adding steric hindrances which prevent off-edge contacts, altogether. In Fig. 5, we depict black, purely repulsive beads that denote the end of an edge and interfere with corner–corner defects, suppressing configurational state 2. These are essentially surrogates for the erased corners. In keeping with the genetic analogy, we term these points "stop codons." These codons do not need to be placed in symmetrically equivalent positions.

Just as the chemical realization of a "point" is system-dependent, so too is the stop codon. We simply consider them to be sterically interfering regions that help the system distinguish edges from corners to help improve self-assembly. If the shape of the colloid is such that it naturally interferes with corner–corner contact, they may be unnecessary. If the edges are encoded with many points, the energetic driving force ($N\varepsilon$) for correct edge–edge contact may also naturally overwhelm the corner–corner energy (2ε), and a good temperature annealing protocol could be used to avoid defects. Annealing protocols were not explored in this work, as they are system-dependent; instead, systems were simply

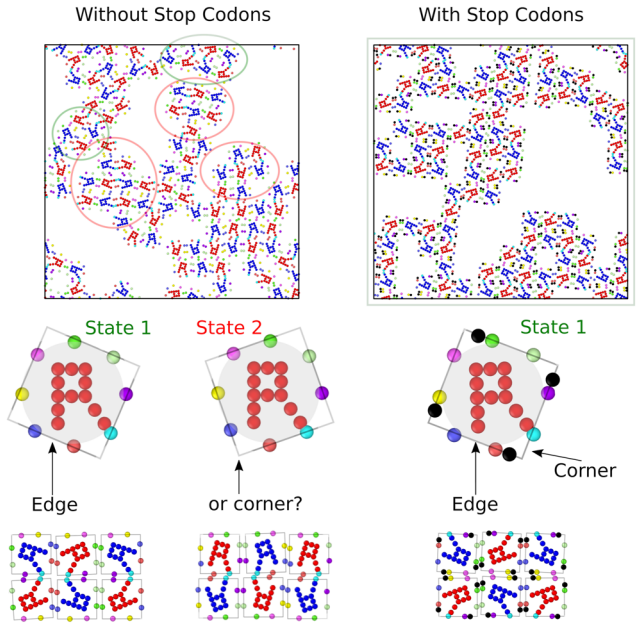

FIG. 6. Example of a colloid functionalized by an inscribing square to form *p*2 mm (*2222) symmetry. Here, only two points are placed along an edge, leading to confusion between what constitutes an edge vs a corner (State 1 vs 2). Simulations were performed at $T^* = 0.125$, $\rho = 0.5$ and run for 2.5×10^8 steps; the final snapshot is shown at the top when stop codons are not (left) and are (right) used. Defects in the case when stop codons are used arise only from the simulation cell being incommensurate with the unit cell dimensions of the crystal.

quenched to low temperature. Figure 6 presents simulations contrasting self-assembly with and without these codons for this example.

Thus, our general guideline is to employ four labeled sites and one stop codon per edge. Each unique point is numbered, with symmetrically equivalent ones assigned the same number. Figure 5(d) illustrates the overall functionalization procedure for three different tiles corresponding to different symmetries. If we ignore the shape and simply read the site identities in a fixed orientation, it becomes clear that different edge symmetry genes confer specific patterns, again akin to those found in biological gene sequences. In this scheme, each edge is separated from its neighbor by a stop codon. A C_x edge results in a palindromic sequence between two neighbors, which we call a "connected palindrome." A pair of T edges are connected by a translation that necessarily dislocates them, resulting in a "disconnected palindrome." Edges related by glides, G_x form repeated sequences. If the glide pairs are connected, as we required in our shortcut method (gapless vertex), then the sequences are connected; this manifests in the genetic sequence as a G_xG_x term [e.g., tile (3) or (17)]. This is not required, however, and they may also be disconnected from each other, as in tile (1) or (9). Finally, mirrored edges, $\overline{A}_x$, manifest as unique sequences since they do not pair with any other edge on the fundamental domain.

Figure 7 shows the results for manually designed colloids, shown schematically alongside representative snapshots from the end of each simulation. The only apparent "defects," which emerge are due to (1) "holes" that could be filled from above the assembly plane if an analogous experiment was carried out by depositing colloids onto an interface or (2) the simulation box being incommensurate with the crystal's unit cell. The latter was chosen purposefully to avoid any bias. These assemblies are crystallographically perfect in the sense that the position and orientation of any colloidal unit are completely determined by the position and orientation of any other. Thus, they form an isohedral tiling, as designed.

B. Robustness and redundancy

It is not always necessary to imprint every letter in a gene sequence on the colloidal unit; at a minimum, enough edges must be present to permit any unit to follow a path by "crossing" the edges (letters) to reach any other unit. This is the concept of a transitivity class; isohedral tiles have only one transitivity class, meaning that any tile can be mapped to any other via group operations, which are encoded by edges.[16] It is sometimes possible that multiple combinations of different moves can provide this transit. For example, in Fig. 8, we present two possible functionalizations for the $CG_1G_2G_1G_2$ gene (*p*2*gg* group). Two possible transits between neighbors along the diagonal are shown: a glide reflection across a red edge, then again across a blue one (indicated in magenta), or one may simply rotate 180° across the green edge. It is, therefore, possible to use only the red and blue edges (Option 2) to induce correct assembly. In fact, any two of the three edge pairs (different color combinations) will work in this case: $[X]G_1G_2G_1G_2$ (red, blue), $C[X]G_2[X]G_2 \rightarrow CGG$ (green, blue), or $CG_1[X]G_1[X] \rightarrow CGG$ again (green, red).

Thus, in many cases, self-assembly is robust against the destruction of a single character in the gene; however, insertion of an incorrect gene might disrupt it, unless the letter is consistent with the group itself, e.g., $[X]G_1G_2G_1G_2 \rightarrow CG_1G_2G_1G_2$. Note that the remaining sequence of letters in this partially deleted gene correspond exactly to another gene in the same wallpaper group. Observe that single deletions always maintain the same wallpaper group, assuming the result is a valid sequence. For example, deleting a T-pair to go from TCTGG → CGG is valid since CGG is a valid tile, whereas deleting the G-pair (TCTGG → TCT) is not since TCT is not a valid gene for any wallpaper group.

Essentially, this implies that the wallpaper group is a conserved quantity under stepwise evolution. Genes in Table I that belong to different groups differ from each other by more than one mutation, whereas all genes that differ by a single mutation belong to the same group. This stepwise evolution corresponds to steps between neighbors in reaction networks, such as Fig. 4.

The partially deleted gene should not be regarded as identical to those genes of the same name, however, since their perimeters form a closed ring, whereas the defective one does not. To recover the original shape from a complete gene, a gap in the ring must be created, then subsequently filled with the correct letter. This "mutation" is analogous to those in biological genes, but it should not be confused with the term "symmetry mutation" used by Huson to describe operations that map one symmetry group to another while not necessarily remaining confined to $\mathbb{E}^2$.[53] The presence of symmetry in biological systems has long been appreciated, but its origin is of some debate. Recently, algorithmic information theory has suggested that, because they require less information to encode,

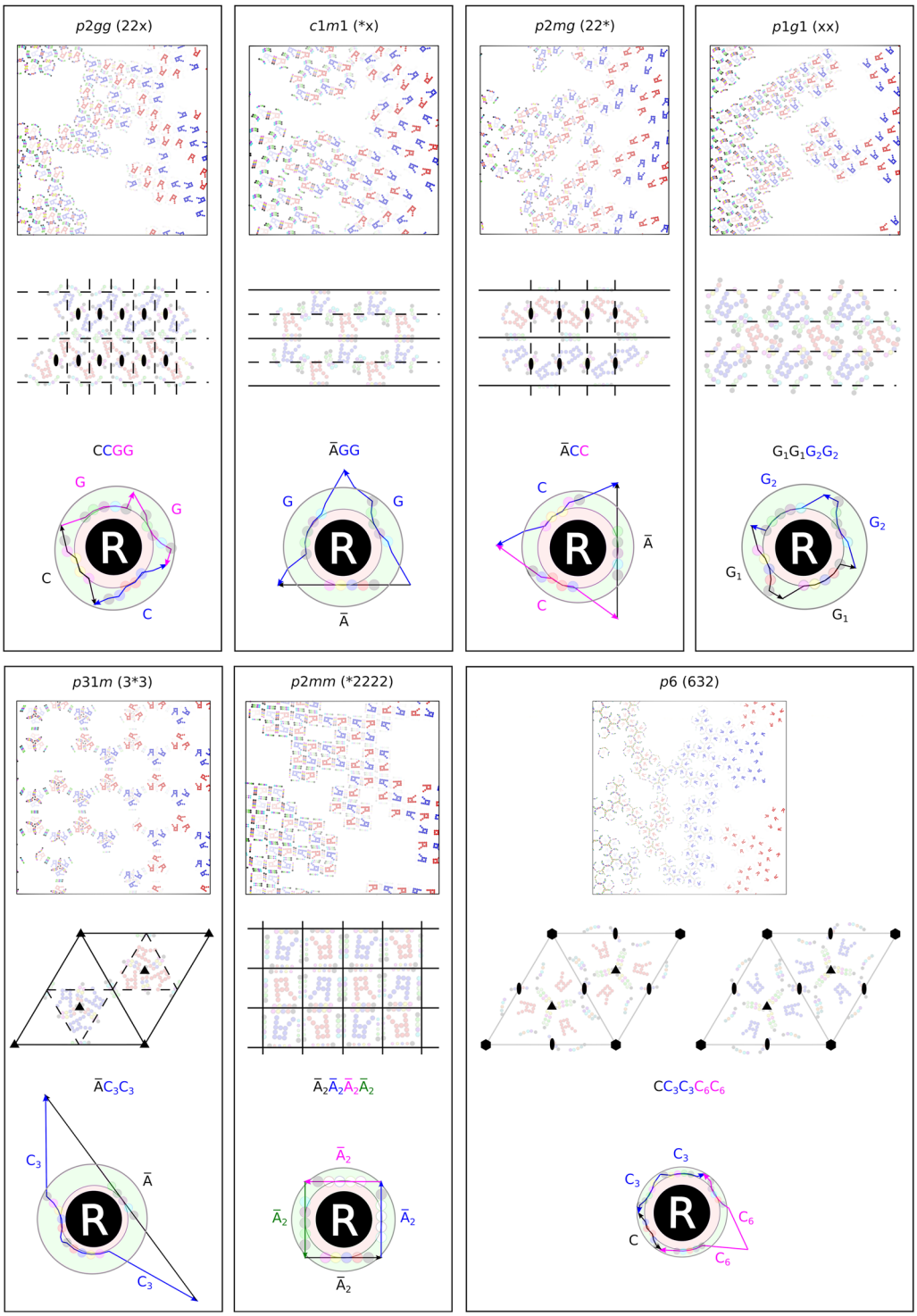

FIG. 7. Examples of functionalized nanoparticles derived from a gene belonging to different wallpaper groups. A simulation snapshot is shown at the top of each box, above a representative portion overlaid with a conventional symmetry diagram, followed by a cartoon illustrating the conversion of the gene to a functionalized corona. Solid black lines denote reflections, dashed ones for glides, ellipses indicate 2-fold rotation, while other N-fold centers are indicated by regular N-gons. Red and blue "R"s have been added as guides to the eye whose colors indicate different chiralities. The example for $p6$ undergoes chiral phase separation as discussed in Ref. 19; unit cells for each phase are shown.

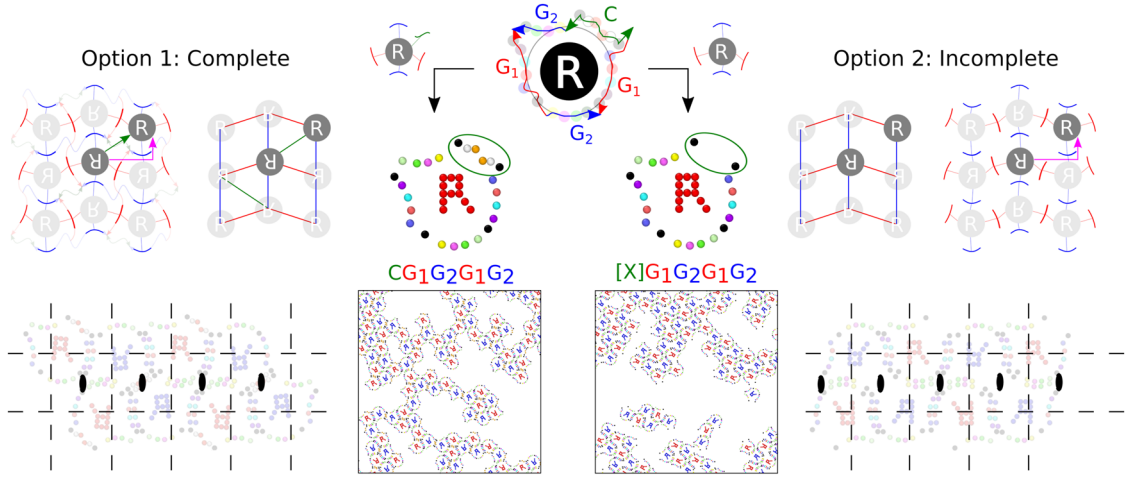

FIG. 8. An example of redundancy in a gene. Option 1 shows a complete encoding of the $CG_1G_2G_1G_2$ gene, whereas Option 2 shows the same functionalization without the C edge ($[X]G_1G_2G_1G_2$). Simulations were performed at $T^* = 0.25$, $\rho = 0.66$ and were run for 2.5×10^8 steps. For Option 1 (left) the twofold rotation center (C) is intact and assembly proceeds until all edges are correctly matched. For Option 2 (right), the rotation center has been removed, yet assembly proceeds essentially just as well because the 180° rotation (green) is equivalent to a composition of the two orthogonal glide reflections (red and blue). Bonding networks are shown on the periphery to illustrate that both systems are connected.

symmetric structures are more likely to occur from random mutations; moreover, lower complexity correlates with higher mutational robustness,[54] which is linked to designability.[55] Darwinian evolution has also recently been designed with artificial self-replicating tiles.[56]

These gene sequences are always self-consistent and, thus, represent some degree of redundancy if there are more letters than necessary. Not all tiles contain redundancies; for example, tile (33) (gene CCC) requires all three edges. The orbifold represents a minimum set of isometries needed to generate a given pattern and our shortcut method uses these explicitly. Therefore, this method conveniently reveals the simplest programming possible by starting from the rings in Fig. 3 and setting as many edge lengths to zero as possible. This results in a tile (gene) with the minimum number of edges needed for each group. For example, the generic starting point for *p2gg* (cf. Fig. 2) is CCGG, where one of the C's may be eliminated to yield CGG.

V. CONCLUSIONS

We presented a method to derive surface functionalization patterns for patchy colloidal systems that induce self-assembly into a structure with a specified wallpaper group. We accomplished this by using isohedral tilings as imprintable "stamps" that define the perimeter of a colloidal object, which correspond to fundamental domains of crystals. By virtue of symmetry, parts of these perimeters are related to each other by the isometries of the plane; this defines allowable shape and chemical bonding patterns. Conveniently, this perimeter may be described by a sequence of letters identical to those of DNA's nucleobases. This suggests an interpretation of these isohedral tiles as a useful inorganic genome for colloidal materials, which may be considered a simplified form of more elaborate genomes of tilings used to describe inorganic materials.[37]

These tiles may contain any asymmetric object, which may be composed of other pre-assembled subunits, turning it into the basic unit of an infinitely periodic tiling. We note that it is possible for very symmetric units to increase the symmetry of the pattern when encompassed by a gene under certain circumstances;[16] however, as in previous work,[19] we regard these as exceptions which will be addressed in the future.

The genetic analogy goes beyond this superficial lettering scheme. It is a useful framework for understanding how the surface functionalization pattern may contain redundancies, repeated or palindromic parts, can be mutated, and may benefit from the use of sterically interfering "stop codons." These tile patterns may be represented by other means, such as incidence symbols as in Ref. 16; however, orbifolds represent a unifying underlying topological concept for symmetry across many spaces and dimensionalities. They offer intuitive interpretations of edge relationships and how different isohedral tiles emerge from the same central surface by "cutting" it into flat pieces.[34,57]

We discussed a simplified approximation of this process, which we anticipate will facilitate its practical application. This simplification results in an incomplete enumeration of tile possibilities, but we have shown how the missing tiles are related to, and emerge by modification of, others. We presented arguments to describe a minimal encoding of this information to further simplify experimental realization.

Various aspects of these patterns have been previously explored by mathematicians and artists, in particular, Heesch and Escher. Here, we have used only simple forms to decorate and assemble colloidal units to avoid distraction from the method; however, Escher's designs of recognizable shapes occupy the opposite end of the design spectrum, which serves to illustrate the broad range of shapes that can be accommodated by this approach. While computational tools may be leveraged, in principle, much of this design may be carried

out by hand (again, as Escher illustrates) since our genetic labeling scheme is an expanded prescriptive variation on Heesch's original system. Seeman cited Escher's work as the original source of inspiration for DNA-nanotechnology,[58] while Escher himself cited the regular division of the plane as the "richest source" of inspiration he ever found.[43] We suggest symmetry-based design is an underutilized approach in the design of colloidal materials where symmetry is often expected to emerge in the final product, rather than being explicitly used as a starting point to design components. In particular, fundamental domains of crystallographic groups serve as rational forward design constructs.

SUPPLEMENTARY MATERIAL

See the supplementary material for additional examples and references on how to construct genes, manipulate them, and transform them into each other. Additional simulations and discussions are also available therein.

ACKNOWLEDGMENTS

Contribution of the National Institute of Standards and Technology (NIST), not subject to U.S. Copyright.

AUTHOR DECLARATIONS

Conflict of Interest

The authors have no conflicts to disclose.

Author Contributions

Nathan A. Mahynski: Conceptualization (lead); Formal analysis (lead); Investigation (lead); Methodology (lead); Software (lead); Supervision (equal); Writing – original draft (lead); Writing – review & editing (equal). **Bliss Han**: Formal analysis (supporting); Investigation (supporting); Methodology (supporting); Writing – review & editing (supporting). **Daniel Markiewitz**: Formal analysis (supporting); Investigation (supporting); Methodology (supporting); Software (supporting); Writing – review & editing (supporting). **Vincent K. Shen**: Resources (lead); Supervision (equal); Writing – review & editing (equal).

DATA AVAILABILITY

The data that support the findings of this study are available from the corresponding author upon reasonable request.

REFERENCES

[1]K. R. Phillips, G. T. England, S. Sunny, E. Shirman, T. Shirman, N. Vogel, and J. Aizenberg, "A colloidoscope of colloid-based porous materials and their uses," Chem. Soc. Rev. **45**, 281–322 (2016).

[2]G. Bonacucina, M. Cespi, M. Misici-Falzi, and G. F. Palmieri, "Colloidal soft matter as drug delivery system," J. Pharm. Sci. **98**, 1–42 (2009).

[3]R. Parthibarajan, C. R. Reichel, N. Gowrishankar, and D. Pranitha, "Colloidosomes drug delivery—A review," Int. J. Pharm. Biol. Sci. **1**, 183–197 (2011); available at https://www.ijpbs.com/previousissue.php?year=2011&issue=3.

[4]S. Wintzheimer, T. Granath, M. Oppmann, T. Kister, T. Thai, T. Kraus, N. Vogel, and K. Mandel, "Supraparticles: Functionality from uniform structural motifs," ACS Nano **12**, 5093–5120 (2018).

[5]N. Skar-Gislinge, M. Ronti, T. Garting, C. Rischel, P. Schurtenberger, E. Zaccarelli, and A. Stradner, "A colloid approach to self-assembling antibodies," Mol. Pharmaceutics **16**, 2394–2404 (2019).

[6]Y. Tian, T. Wang, W. Liu, H. L. Xin, H. Li, Y. Ke, W. M. Shih, and O. Gang, "Prescribed nanoparticle cluster architectures and low-dimensional arrays built using octahedral DNA origami frames," Nat. Nanotechnol. **10**, 637–644 (2015).

[7]W. Liu, J. Halverson, Y. Tian, A. V. Tkachenko, and O. Gang, "Self-organized architectures from assorted DNA-framed nanoparticles," Nat. Chem. **8**, 867–873 (2016).

[8]W. Wang, S. Chen, B. An, K. Huang, T. Bai, M. Xu, G. Bellot, Y. Ke, Y. Xiang, and B. Wei, "Complex wireframe DNA nanostructures from simple building blocks," Nat. Commun. **10**, 1067 (2019).

[9]Y. Tian, J. R. Lhermitte, L. Bai, T. Vo, H. L. Xin, H. Li, R. Li, M. Fukuto, K. G. Yager, J. S. Kahn, Y. Xiong, B. Minevich, S. K. Kumar, and O. Gang, "Ordered three-dimensional nanomaterials using DNA-prescribed and valence-controlled material voxels," Nat. Mater. **19**, 789–796 (2020).

[10]Z. Lin, H. Emamy, B. Minevich, Y. Xiong, S. Xiang, S. Kumar, Y. Ke, and O. Gang, "Engineering organization of DNA nano-chambers through dimensionally controlled and multi-sequence encoded differentiated bonds," J. Am. Chem. Soc. **142**, 17531–17542 (2020).

[11]M. Rechtsman, F. Stillinger, and S. Torquato, "Designed interaction potentials via inverse methods for self-assembly," Phys. Rev. E **73**, 011406 (2006).

[12]D. Chen, G. Zhang, and S. Torquato, "Inverse design of colloidal crystals via optimized patchy interactions," J. Phys. Chem. B **122**, 8462–8468 (2018).

[13]Z. M. Sherman, M. P. Howard, B. A. Lindquist, R. B. Jadrich, and T. M. Truskett, "Inverse methods for design of soft materials," J. Chem. Phys. **152**, 140902 (2020).

[14]B. A. Lindquist, "Inverse design of equilibrium cluster fluids applied to a physically informed model," J. Chem. Phys. **154**, 174907 (2021).

[15]T. Vo and S. C. Glotzer, "A theory of entropic bonding," Proc. Natl. Acad. Sci. U. S. A. **119**, e2116414119 (2022).

[16]B. Grünbaum and G. C. Shepherd, *Tilings and Patterns* (Dover Publications, 2016).

[17]H. Heesch and O. Kienzle, *Flächenschluß: System der Formung lückenlos aneinanderschliessender Flachteile* (Springer, Berlin, 1963).

[18]D. Schattschneider, "The plane symmetry groups: Their recognition and notation," Am. Math. Mon. **85**, 439–450 (1978).

[19]N. A. Mahynski and V. K. Shen, "Symmetry-derived structure directing agents for two-dimensional crystals of arbitrary colloids," Soft Matter **17**, 7853–7866 (2021).

[20]J. E. Padilla, C. Colovos, and T. O. Yeates, "Nanohedra: Using symmetry to design self assembling protein cages, layers, crystals, and filaments," Proc. Natl. Acad. Sci. U. S. A. **98**, 2217–2221 (2001).

[21]I. G. Denisov, Y. V. Grinkova, A. A. Lazarides, and S. G. Sligar, "Directed self-assembly of monodisperse phospholipid bilayer nanodiscs with controlled size," J. Am. Chem. Soc. **126**, 3477–3487 (2004).

[22]T. Sawada and M. Fujita, "Folding and assembly of metal-linked peptidic nanostructures," Chem **6**, 1861–1876 (2020).

[23]E. Winfree, F. Liu, L. A. Wenzler, and N. C. Seeman, "Design and self-assembly of two-dimensional DNA crystals," Nature **394**, 539–544 (1998).

[24]P. W. K. Rothemund, N. Papadakis, and E. Winfree, "Algorithmic self-assembly of DNA Sierpinski triangles," PLoS Biol. **2**, e424 (2004).

[25]Y. Wang, Y. Wang, D. R. Breed, V. N. Manoharan, L. Feng, A. D. Hollingsworth, M. Weck, and D. J. Pine, "Colloids with valence and specific directional bonding," Nature **491**, 51–55 (2012).

[26]F. Praetorius and H. Dietz, "Self-assembly of genetically encoded DNA-protein hybrid nanoscale shapes," Science **355**, eaam5488 (2017).

[27]Y. Xiong, S. Yang, Y. Tian, A. Michelson, S. Xiang, H. Xin, and O. Gang, "Three-dimensional patterning of nanoparticles by molecular stamping," ACS Nano **14**, 6823–6833 (2020).

[28]F. J. Rizzuto, T. Trinh, and H. F. Sleiman, "Molecular printing with DNA nanotechnology," Chem **6**, 1560–1574 (2020).
[29]J. F. Reuther, S. D. Dahlhauser, and E. V. Anslyn, "Tunable orthogonal reversible covalent (TORC) bonds: Dynamic chemical control over molecular assembly," Angew. Chem., Int. Ed. **58**, 74–85 (2019).
[30]W. P. Thurston, *The Geometry and Topology of Three-Manifolds* (Princeton University, Princeton, NJ, 1979).
[31]J. H. Conway, "The orbifold notation for surface groups," in *Groups, Combinatorics and Geometry: Proceedings of the L.M.S. Durham Symposium*, London Mathematical Society Lecture Note Series Vol. 165 (Cambridge University Press, Cambridge, 1992), pp. 438–447.
[32]J. H. Conway and D. H. Huson, "The orbifold notation for two-dimensional groups," Struct. Chem. **13**, 247–257 (2002).
[33]D. H. Huson, "The generation and classification of tile-*k*-transitive tilings of the euclidean plane, the sphere and the hyperbolic plane," Geometriae Dedicata **47**, 269–296 (1993).
[34]J. H. Conway, H. Burgiel, and C. Goodman-Strauss, *The Symmetries of Things* (CRC Press, 2016).
[35]S. T. Hyde, S. J. Ramsden, and V. Robins, "Unification and classification of two-dimensional crystalline patterns using orbifolds," Acta Crystallogr., Sect. A **70**, 319–337 (2014).
[36]C. K. Johnson, M. N. Burnett, and W. D. Dunbar, "Crystallographic topology and its applications," Crystallogr. Comput. **7**, 1–25 (1996); available at https://www.osti.gov/biblio/392732.
[37]O. Delgado-Friedrichs, S. T. Hyde, M. O'Keeffe, and O. M. Yaghi, "Crystal structures as periodic graphs: The topological genome and graph databases," Struct. Chem. **28**, 39–44 (2017).
[38]S. J. Chung, T. Hahn, and W. E. Klee, "Nomenclature and generation of three-periodic nets: The vector method," Acta Crystallogr., Sect. A **40**, 42–50 (1984).
[39]O. D. Friedrichs, A. W. M. Dress, D. H. Huson, J. Klinowski, and A. L. Mackay, "Systematic enumeration of crystalline networks," Nature **400**, 644–647 (1999).
[40]M. D. Foster, A. Simperler, R. G. Bell, O. D. Friedrichs, F. A. A. Paz, and J. Klinowski, "Chemically feasible hypothetical crystalline networks," Nat. Mater. **3**, 234–238 (2004).
[41]N. W. Ockwig, O. Delgado-Friedrichs, M. O'Keeffe, and O. M. Yaghi, "Reticular chemistry: Occurrence and taxonomy of nets and grammar for the design of frameworks," Acc. Chem. Res. **38**, 176–182 (2005).
[42]H.-G. Bigalke and H. Wippermann, *Reguläre Parkettierungen* (B.I. Wissenschaftsverlag, Mannheim, 1994).
[43]D. Schattschneider, *Visions of Symmetry* (Abrams, 2004).
[44]M. C. Escher, *Regelmatige Vlakverdeling* (De Roos, 1958).
[45]D. Kazanci and A. Vince, "A property of normal tilings," Am. Math. Mon. **111**, 813–816 (2004).
[46]D. Frenkel and B. Smit, *Understanding Molecular Simulation: From Algorithms to Applications*, Computational Science Series Vol. 1, 2nd ed. (Academic Press, 2001).
[47]C. S. Kaplan, "Metamorphosis in Escher's art," in *Bridges Leeuwarden: Mathematics, Music, Art, Architecture, Culture*, edited by R. Sarhangi and C. H. Séquin (Tarquin Publications, London, 2008), pp. 39–46, available online at http://archive.bridgesmathart.org/2008/bridges2008-39.html.
[48]W. W. Chow, "Automatic generation of interlocking shapes," Comput. Graphics Image Process. **9**, 333–353 (1979).
[49]S. Plimpton, "Fast parallel algorithms for short-range molecular dynamics," J. Comput. Phys. **117**, 1–19 (1995).
[50]S. Toxvaerd and J. C. Dyre, "Communication: Shifted forces in molecular dynamics," J. Chem. Phys. **134**, 081102 (2011).
[51]M. Daoud and J. P. Cotton, "Star shaped polymers: A model for the conformation and its concentration dependence," J. Phys. **43**, 531–538 (1982).
[52]V. Pryamtisyn, V. Ganesan, A. Z. Panagiotopoulos, H. Liu, and S. K. Kumar, "Modeling the anisotropic self-assembly of spherical polymer-grafted nanoparticles," J. Chem. Phys. **131**, 221102 (2009).
[53]D. H. Huson, Two-dimensional symmetry mutation, http://citeseerx.ist.psu.edu/viewdoc/download?doi=10.1.1.30.8536&rep=rep1&type=pdf; accessed 16 September 2021.
[54]I. G. Johnston, K. Dingle, S. F. Greenbury, C. Q. Camargo, J. P. Doye, S. E. Ahnert, and A. A. Louis, "Symmetry and simplicity spontaneously emerge from the algorithmic nature of evolution," Proc. Nat. Acad. Sci. **119**(11), e2113883119 (2022).
[55]T. Wang, J. Miller, N. S. Wingreen, C. Tang, and K. A. Dill, "Symmetry and designability for lattice protein models," J. Chem. Phys. **113**, 8329–8336 (2000).
[56]F. Zhou, R. Sha, H. Ni, N. Seeman, and P. Chaikin, "Mutations in artificial self-replicating tiles: A step toward Darwinian evolution," Proc. Natl. Acad. Sci. U. S. A. **118**, e2111193118 (2021).
[57]J. H. Conway, O. Delgado Friedrichs, D. H. Huson, and W. Thurston, "On three-dimensional space groups," Contrib. Algebra Geom. **42**, 475–507 (2001).
[58]N. C. Seeman, "Nucleic acid nanostructures and topology," Angew. Chem., Int. Ed. **37**, 3220–3238 (1998).